Chapter 5

In vitro overexpression of CHAPa and CHAPb in mouse cardiomyocytes and skeletal muscle cells interferes with Z-disc integrity and decreases fetal gene expression

Willemijn van Eldik, Abdelaziz Beqqali, Jantine Monshouwer-Kloots,
Twan de Vries, Christine Mummery, Robert Passier

Abstract

In the previous chapter we have described that CHAPb transgenic mice displayed features of cardiomyopathy and cardiac dysfunction, whereas CHAPa transgenic mice did not display any abnormalities. In order to determine direct effects of both CHAP isoforms, we infected mouse cardiomyocytes (E17.5) and skeletal muscle cells myoblast cells (C2C12) with adenoviral constructs for CHAPa and CHAPb.
In vitro overexpression of CHAPa resulted in Z-disc disruption, as shown by α-actinin-2 staining in both C2C12 cells and cardiomyocytes. CHAPb overexpression in C2C12 and cardiomyocytes resulted in stress fiber formation, which stained for F-actin. Although RhoA and phosphorylated Ezrin/Moesin/Radixin, proteins involved in linking the actin cytoskeleton to the plasma membrane, were ectopically expressed in cardiomyocytes, no activation of the actin signaling pathway was observed. Surprisingly, in both CHAPa and CHAPb infected cells downregulation of hypertrophy markers *Nppa*, *Nppb* and *Myh7* was observed, whereas *Myh6* was upregulated. In agreement with these findings we observed that a key player in muscle hypertrophy and development, the transcription factor Nuclear Factor of Activated T-cells-c2 (NFATc2), was translocated from the nucleus to the cytoplasm. These results show that CHAPa and CHAPb have an important role in maintaining the integrity of muscle cells. Furthermore, interestingly our findings suggest that CHAPa and b isoforms may directly affect transcriptional regulation regarding maturation and/or blocking hypertrophy of cardiomyocytes.

Introduction

Cardiac hypertrophy is a compensatory mechanism of the heart to increased workload as a result of loss of cardiomyocytes that occurs in pathophysiological events (for example myocardial infarction). During a hypertrophic response cardiomyocytes increase their cell volume to compensate for the loss of cardiomyocytes. Cardiomyocytes respond to stress by expressing a specific subset of fetal genes, such as Atrial Natriuretic Factor (ANF), Brain Natriuretic Peptide (BNP) and β-Myosin Heavy Chain (β-MHC), leading to the described hypertrophic response[1-3]. The basic contractile unit of cardiomyocytes is the sarcomere, which is delineated by the Z-disc[4], which consists of a protein complex, including α-actinin-2 and CHAP. Z-disc proteins may sense stress signals, and activate signaling pathways leading to activation of the fetal gene program[5, 6].In the previous chapters we have seen that CHAP is expressed in skeletal and heart muscle cells during embryonic development and in adulthood. Two isoforms of CHAP exists: CHAPa is the longest isoform and contains a PDZ domain and nuclear localization signal (NLS), whereas the shorter isoform CHAPb lacks the PDZ domain. Whereas CHAPa is predominantly expressed in adult tissues, CHAPb is expressed at higher levels in the developing heart and muscles[7]. CHAP is homologous to synaptopodin and myopodin, which have both been implicated in actin signaling. Myopodin is expressed in the Z-disc of cardiac and skeletal muscle and interacts with α-actinin-2[8]. Synaptopodin interacts with α-actinin-2 and -4[11], and is involved in actin signaling in kidney podocytes by the formation of actin stress fibers via RhoA[12].

Besides localization at the Z-disc, Myopodin is also able to translocate to the nucleus, which is mediated by 14-3-3[9].It has been shown that interaction between 14-3-3 and Myopodin can be regulated by various kinases and phosphatases, such as Protein Kinase A (PKA), $Ca2^{+}$/calmodulin-dependent kinase II (CaMKII) and the phosphotase calcineurin, a key player in cardiac hypertrophy[10].

In the previous chapter, we described the phenotypes of heart-specific CHAPa- and b transgenic (Tg) mice. CHAPa Tg mice did not show a phenotype after one year of age or after myocardial infarction (Chapter 4 and data not shown), although misfolding or partially degradation could not be excluded. CHAPb Tg mice, on the other hand developed features of cardiomyopathy, including cardiac hypertrophy and diastolic dysfunction. Furthermore, stress fibers were apparent in CHAPb Tg hearts which was associated with activation of the actin signaling pathway.

To study the direct effects of CHAP we induced expression for both isoforms by adenoviral transduction in skeletal muscle cells (C2C12) and embryonic 17.5 (E17.5) mouse cardiomyocytes. We found that CHAPa- and b both disrupted the Z-disc structure of cardiomyocytes and differentiated C2C12 cells. However, only CHAPb induced stress fibers, similar to the stress fibers found in CHAPb Tg hearts. In contrast to the CHAPb Tg hearts we did not observe a significant upregulation of the actin signaling and reactivation of fetal cardiac genes, a hallmark of pathological cardiac hypertrophy. In fact, we observed an opposite effect on re-expression of fetal cardiac genes, which included a switch in expression of MHC isoforms and downregulation of ANF and BNP. These changes were further accompanied by translocation of Nuclear Factor of Activated T-cells (NFAT), suggesting that direct effects of CHAP may be involved in further maturation of muscle cells or even have anti-hypertrophic effect on striated muscle cells.

Materials and methods

Animals and cardiomyocyte isolation
Swiss mice were intercrossed for collection of embryos at embryonic day 17.5 (E17.5). Embryos were collected and rinsed in PBS. Hearts were removed and rinsed in PBS. Subsequently, hearts were rotated over night in 1x trypsin/EDTA (Sigma-Aldrich Chemie). The next day trypsin/EDTA was removed by transferring hearts over a 70 µm strainer (BD Biosciences). In a next step, cardiomyocytes were isolated by shaking the hearts in fractions of collagenase mix (0.5 ml 22% BSA (Sigma-Aldrich Chemie) and 15 µl Collagenase type 1A (36.9 u/µl; Sigma-Aldrich Chemie) in 30 ml 0.9% NaCl for 3 minutes at 37 °C. After each fraction, hearts were put over a new 70 µm strainer (BD Biosciences) and filtered. Each fraction was collected in 2 ml fetal calf serum (FCS, Sigma-Aldrich Chemie), followed by rinsing the strainer with 5 ml cardiomyocyte medium (Dulbecco's Modified Eagle Medium F12 [DMEM F12, Invitrogen], 15% FCS and pen/strep [Invitrogen]). The remainder of the hearts was put in a new fraction with collagenase mix and the procedure was applied until all hearts were dissolved. All fractions were collected, cells were spun down, resuspended in new cardiomyocyte medium and finally cells were counted and plated on gelatin-coated dishes. The amount of cells plated was 75,000 per 24-well and 380,000 per 6-well. The next day medium was refreshed with cardiomyocyte medium without FCS.

Cell culture
First-generation human adenovirus type 5 (HAdV5) vectors were produced in PER.tTA. Cre76 cells[13]. These HAdV5 early region 1 (E1)-transformed human embryonic retinoblasts were maintained in DMEM (Invitrogen) containing 10% fetal bovine serum (FBS; Invitrogen) and 10 mM $MgCl_2$ and cultured at 37°C in a humidified atmosphere of 90% air and 10% CO_2. Endpoint titrations of HAdV5 vector preparations were carried out in HeLa cells, which were fed DMEM containing 5% FCS (Sigma Aldrich). C2C12 cells were cultured in DMEM with 10% FCS and pen/strep added. For differentiation of C2C12 cells, cells were incubated with DMEM with 2% horse serum (Invitrogen) and pen/strep added. Medium was refreshed every other day.
The latter cell types were cultured at 37°C in a humidified atmosphere of 95% air and 5% CO_2.

Generation of first-generation HAdV5 vectors encoding murine CHAP isoforms a and b.
The codinq sequences of murine CHAPa and CHAPb were amplified by Platinum Taq DNA Polymerase High fidelity (Invitrogen) polymerase chain reaction from cDNA templates that were generated earlier[7] using the forward primers 5'-GCGGCCGCCCACC**ATG**GGTGCTGAGGAGGAGGT-3' and 5'-GCGGCCGCCCACC**ATG**GAGACCACCATCCAAGA-3', respectively, together with a single reverse primer (5'-GTCGACACTGGTGCCCTGCCCC-3'), the stopcodon was included in a c-terminal flag-tag. The amplification products were subcloned into pCRII (Invitrogen) and subjected to nucleotide sequence analysis. The pShuttle-IRES-hrGFP-1 vector was used for generating adenoviruses of CHAPa (AdCHAPa) and CHAPb (AdCHAPb). This vector contains a CMV promoter, a multiple cloning site which is followed by internal ribosome entry site (IRES), which directs the translation of human recombinant Green Fluorescent Protein (hrGFP) as a second open reading frame. Errorless coding sequences of murine CHAPa and CHAPb were transferred to pShuttle-IRES-hrGFP-1 (Agilent

Technologies) using NotI and SalI to produce pShuttle-mCHAPa-IRES-hrGFP-1 and pShuttle-mCHAPb-IRES-hrGFP-1, respectively. These two HAdV5 shuttle constructs were linearized with PmeI and used in combination with pAdEasy-1 DNA for the generation by *in vivo* recombineering[14] of plasmids pAdEasy-1-mCHAPa-IRES-hrGFP-1 and pAdEasy-1-mCHAPb-IRES-hrGFP-1 carrying full-length HAdV5 vector genomes. Following treatment with PacI to release the HAdV5 vector termini, pAdEasy-1-mCHAPa-IRES-hrGFP-1 and pAdEasy-1-mCHAPb-IRES-hrGFP-1 DNA was individually transfected with the aid of linear 25-kDa polyethyleneimine (Polysciences) into PER.tTA.Cre76 cells[13] to produce seed stocks of AdEasy-1-mCHAPa-IRES-hrGFP-1 and AdEasy-1-mCHAPb-IRES-hrGFP-1, respectively. These seed stocks were used for large-scale production of both HAdV5 vectors in PER.tTA.Cre76 cells essentially as described by Gonçalves *et al.*[13]. The functional titers of the resulting AdEasy-1-mCHAPa-IRES-hrGFP-1 and AdEasy-1-mCHAPb-IRES-hrGFP-1 vector preparations were determined by limiting dilution assays in HeLa cells using flow cytometric analysis of *hrGFP-1* expression as readout and were expressed in terms of HeLa cell-transducing units (HTU)/ml. An adenovirus expressing GFP only was used as control and is described in Knaän-Shanzer et al[15].

Infection of cells

Cells were infected with multiplicity of infection (MOI) of 10. After 6-12 hours medium was refreshed. Then cells were left for 24 hours, 48 hours or 7 days.

Immunofluorescence

Cells were grown on gelatin coated coverslips. Cells were washed with PBS and fixed for 30 minutes in 2% PFA at room temperature, followed by 3 washes in PBS. Cells were permeabilized with 0.1% Triton-x-100 in PBS for 8 minutes. Cells were washed 3 times with PBS and blocked for 1 hour in 4% normal goat serum (Vector labs) in PBS. First antibody was applied over night at 4 °C in PBS/normal goat serum. Antibodies used were anti-CHAP (1:50), anti-α-actinin (1:800, Sigma-Aldrich Chemie), myomesin (1:50, kind gift from E. Ehler), anti-RhoA (1:100, Santa Cruz), anti-phosphorylated Ezrin/Moesin/Radixin (1:50, Cell Signaling Technology) or anti-NFATc2 (1:50, G1 D10, Santa Cruz). The next day cells were washed 3 times with PBS/0.05% Tween-20 (PBS-T) for 10 minutes. Secondary antibodies were dissolved in 4% normal goat serum/PBS. Antibodies used were Alexa Fluor® 647 donkey anti-rabbit IgG (1:100, Invitrogen), goat anti-mouse/IgG(H+L)/Cy3 (1:250, Jackson Immuno research). Cells were 3 times washed in PBS-T for 20 minutes, and then 1 time in PBS. F-actin fibers were stained using Alexa555 conjugated phalloidin (1:100, Invitrogen). Cells were counter stained with DAPI for 8 minutes. Coverslips were enclosed with Molviol. Immunofluorescent stainings were analyzed with SP5 confocal microscope (Leica).

Protein isolation and western blot

For protein isolation cells were grown on 6 well plates. Cells were infected and 24 hours, 48 hours or 7 days later protein was isolated (see previous section). For this cells were washed twice with PBS. Then 250 µl ice-cold RIPA buffer (50 mM Tris-HCl pH8, 150 mM NaCl, 1% NP-40 (Sigma-Aldrich Chemie), 0.2% sodium deoxycholate and 0.1% SDS) with extra added protein inhibitors (protease inhibitor cocktail tablets (10 µg/ml; Roche, Germany), 0.1 mmol/L dithiothreitol (DTT; Invitrogen) and 1 mmol/L phenylmethanesulfonylfluoride (PMSF; Sigma Aldrich), 5 mmol/L NaF and 1 mmol/L Na_3VO_4) was added to the cells, which

were then left on ice for 15 minutes. Then cells were scraped on ice and transferred to an eppendorf tube. Lysed cells were spun down (10000 g, 4 °C, 15 minutes) and supernatant was transferred to a new tube. Protein concentration was measured with the Bradford assay (Bio-rad) using bovine serum albumin (BSA) for a standard curve. Then 5x sample buffer (100 mM Tris-HCl pH 6.8, 10% SDS, 50% glycerol, 25% β-mercaptoethanol and bromphenol blue) was added and samples were boiled for 5 minutes at 95 °C. Protein gels were loaded with 30 µg protein. Gels were blotted (Hybond-P, GE healthcare) for 3 hours at room temperature and blocked for one hour with 5% milk/Tris Buffered Saline-tween (TBS-T: 50mM Tris-HCl pH 7.5, 125 mM NaCl, 0.02% Tween-20). First antibody diluted in 5% milk/TBS-T (unless stated else) was applied over night at 4 °C. Antibodies used were anti-RhoA (1:200, Santa Cruz), anti-actin (1:1000, Millipor), anti-α-actinin (1:1000, Sigma-Aldrich Chemie), anti-Ezrin/moesin/radixin (1:1000 in 5% BSA/TBS-T, Cell Signaling Technology), anti-Flag (1:5000, Sigma-Aldrich Chemie) and anti-GAPDH (1:10000, Millipor). Secondary antibody was applied for 1 hour at room temperature. Secondary antibodies used were anti-mouse IgG HRP (1:1000, Cell Signaling Technology) or anti-rabbit IgG HRP (1:2000, Cell Signaling Technology) dissolved in 5% milk/TBS-T. Blots were visualized by using SuperSignal West Pico Chemiluminescent Substrate (Pierce).

RNA isolation and cDNA synthesis

Infected cells were grown in 6 well plates, washed twice with PBS and dissolved in Trizol (Invitrogen). Then RNA was isolated according to the manufactures protocol. RNA was treated with DNase (DNA-free, Ambion) and subsequently translated in cDNA (iScript, BioRad). qPCR analysis was done using the CFX96 Real-Time PCR detection system (Bio-Rad). Primers used are listed in table in the Material and Method section of chapter 4, except for *Myh6*: 5'- CTTCATCCATGGCCAATTCT-3' and 5'- GCGCATTGAGTTCAAGAAGA-3'. Data were analyzed with Bio-Rad CFX Manager.

Results

Generation of adenoviral CHAP constructs

To study the effects of overexpression of CHAPa- and b *in vitro*, we generated adenoviruses encoding flag-tagged CHAPa or –b cDNA (AdCHAPa and AdCHAPb, with additional IRES-GFP expression). An adenovirus expressing GFP (AdGFP) only was used as control. We first investigated the expression of the CHAP adenoviruses in mouse E17.5 cardiomyocytes. For this, cells were infected with AdGFP, AdCHAPa, AdCHAPb and non-infected cells were used as control. After 2 days RNA and protein samples were obtained and expression levels were analyzed with qPCR and western blot. We found a robust overexpression by qPCR for both *ChapA* (Figure 1A) and *ChapB* (Figure 1B) when compared to control virus and the non-infected endogenous CHAP isoforms. Also at the protein level the products of CHAPa and CHAPb could be detected with a flag antibody (Figure 1C), whereas no bands could be detected in the control samples. These results show a specific, robust and stable overexpression of both CHAPa and CHAPb isoforms.

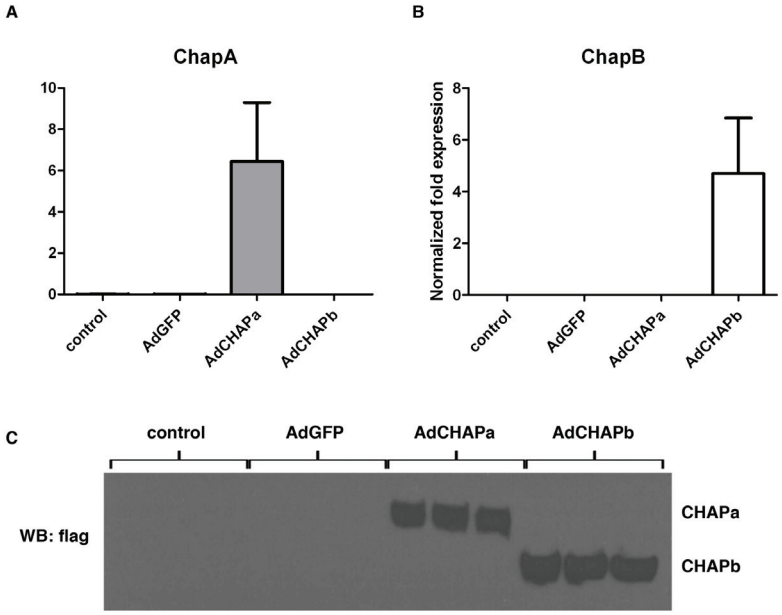

Figure 1: Generation of AdCHAPa and AdCHAPb viruses. Mouse cardiomyocytes were infected with AdCHAPa or Ad-CHAPb. A+B) Expression of *ChapA* (A) or *ChapB* (B) was analyzed by qPCR, *Gapdh*, *H2A* and *Pgk* were used as internal controls. C) Western blot stained with flag antibody shows overexpression of CHAPa and CHAPb at the protein level.

Overexpression of CHAP affects Z-disc organization in both skeletal muscle cells and cardiomyocytes

Next, we studied the role of CHAP in skeletal and heart muscle cells *in vitro*. In chapter 3 we have seen that CHAP is expressed in developing and adult skeletal muscle cells of mouse and chick embryos (see chapter 3). To investigate the role of CHAPa and CHAPb in skeletal muscle differentiation we used a mouse myoblast cell line, C2C12, which can be differentiated to skeletal muscle cells by culturing cells in media containing 2% horse serum. This results in

the formation of multinucleated twitching myotubes in which striations can be detected by α-actinin-2 staining. C2C12 cells were infected with AdGFP, AdCHAPa or AdCHAPb, after the infection medium was replaced for differentiation medium and cells were differentiated for 6 days. Then cells were stained for CHAP and α-actinin-2. The control AdGFP-infected cells formed multinucleated myotubes and striations could be detected in these myotubes with α-actinin-2 staining (Figure 2, upper panels, arrows). However, formation of multinucleated myotubes was disrupted in both AdCHAPa and AdCHAPb infected cells (Figure 2, middle and lower panels). Whereas in AdCHAPa infected cells only the sarcomere structure was disrupted (arrows in middle panel, Figure 2), in AdCHAPb cells additional stress fibers were formed (arrows in lower panel, Figure 2). In undifferentiated C2C12 cells overexpression of CHAPb also induced stress fibers (data not shown).

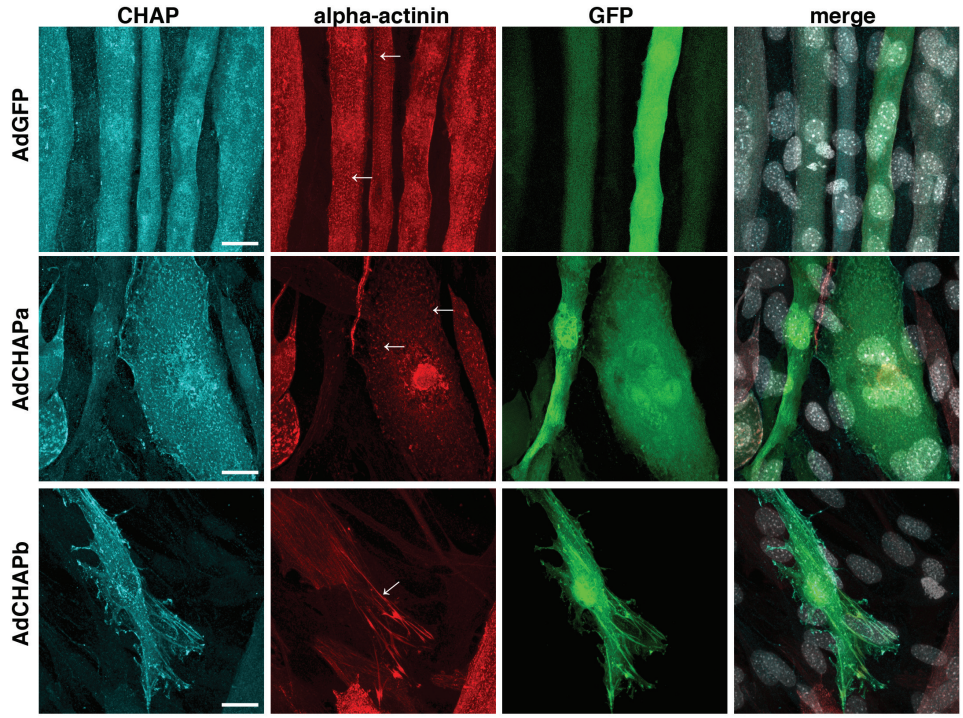

Figure 2: Overexpression of CHAPa and CHAPb affects skeletal muscle differentiation. C2C12 cells were infected with AdGFP, AdCHAPa or AdCHAPb, differentiated and stained for α-actinin-2 (red) and CHAP (cyan). Infected cells can be identified by GFP signal (green), nuclei are stained gray, merge images are shown. In AdGFP infected cells (upper panels) multinucleated myotubes were formed, in which striations could be detected by α-actinin-2 staining (arrows). In AdCHAPa infected cells no multinucleated myotubes were formed and Z-disc was disrupted, which was shown by α-actinin-2 staining (middle panels, arrows). In AdCHAPb infected cells no myotubes were formed, instead, stress fibers were formed, that stained for α-actinin-2 and CHAP (lower panel, arrow).

Next, we investigated overexpression of AdCHAPa and AdCHAPb in E17.5 cardiomyocytes. In CHAPb Tg mice overexpression of CHAPb induces stress fibers, which co-stained for α-actinin-2 and not for myomesin. In AdGFP infected cells CHAP co-localized in the Z-disc with α-actinin-2 (Figure 3A, upper panels) and not with myomesin (Figure 3B, upper panels), which is in agreement with our previous findings[7]. Infection of E17.5 cardiomyocytes with AdCHAPa resulted in disruption of Z-disc structure, which was apparent by both CHAP

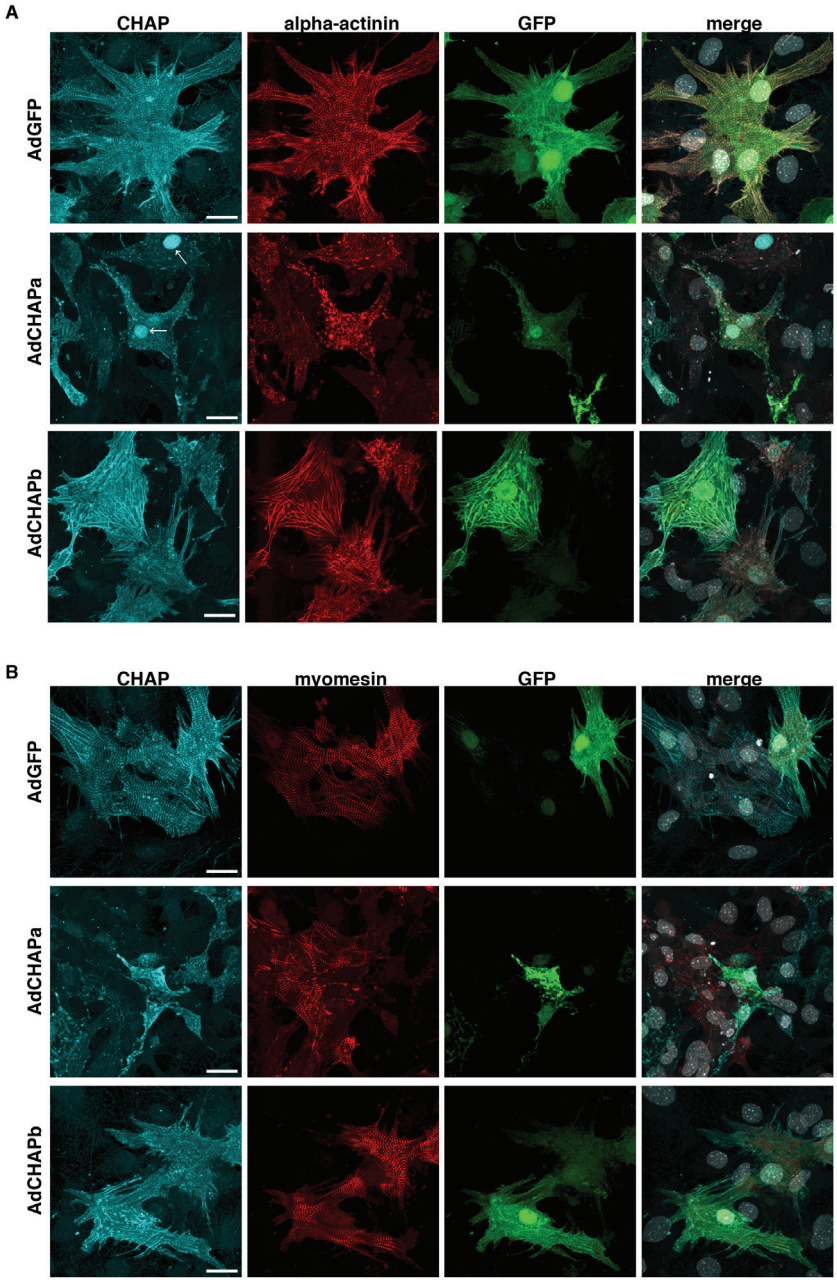

Figure 3: Overexpression of CHAPa and CHAPb results in distinct phenotypes in E17.5 mouse cardiomyocytes. Mouse cardiomyocytes were infected with AdGFP, AdCHAPa or AdCHAPb and stained for α-actinin-2 (red)/CHAP (cyan, A) or Myomesin (red)/CHAP (cyan, B). Infected cells can be identified by GFP signal (green), nuclei are stained gray, merge images are shown. In AdGFP infected cardiomyocytes CHAP localizes at the Z-disc with α-actinin (A, upper panels) and not with myomesin (B, upper panels). In AdCHAPa infected cardiomyocytes the Z-disc is disrupted (A, middle panels, α-actinin), while the m-band is not affected (B, middle panels, myomesin). In AdCHAPb infected cells stress fibers are formed that stain for α-actinin-2 (A, lower panels), while myomesin is not affected (B, lower panels).

and α-actinin-2 staining (Figure 3A, middle panels). Occasionally, infection of AdCHAPa in E17.5 mouse cardiomyocytes resulted in nuclear localization of CHAP (Figure 3A, middle panel, arrows). Infection of E17.5 cardiomyocytes with AdCHAPb resulted in the formation of stress, which stained for CHAP and α-actinin-2 (Figure 3A, lower panels). Staining for myomesin showed that in both AdCHAPa and AdCHAPb infected cells the M-band structure was not affected (Figure 3B, middle and lower panels). Thus formation of stress fibers in AdCHAPb infected cells led to a subsequent loss of Z-disc integrity, whereas the M-band was unaffected. In summary, both CHAP isoforms led to sarcomeric disruption, whereas formation of stress fibers was only evident in AdCHAPb infected cardiomyocytes.

CHAP does not directly affect actin signaling in is not affected in muscle cells

To investigate if the fibers in cells with CHAPb were F-actin fibers, we stained the cells for F-actin (phalloidin) and co-stained for α-actinin-2. In AdGFP infected E17.5 cardiomyocytes phalloidin had a sarcomeric staining pattern (Figure 4, upper panel, arrows). In AdCHAPa infected cells a disrupted pattern for F-actin was observed (Figure 4, middle panel, arrows) and in AdCHAPb infected cells phalloidin indeed stained the fibers, which co-stained for α-actinin-2. These results show that CHAPb induces actin stress fibers.

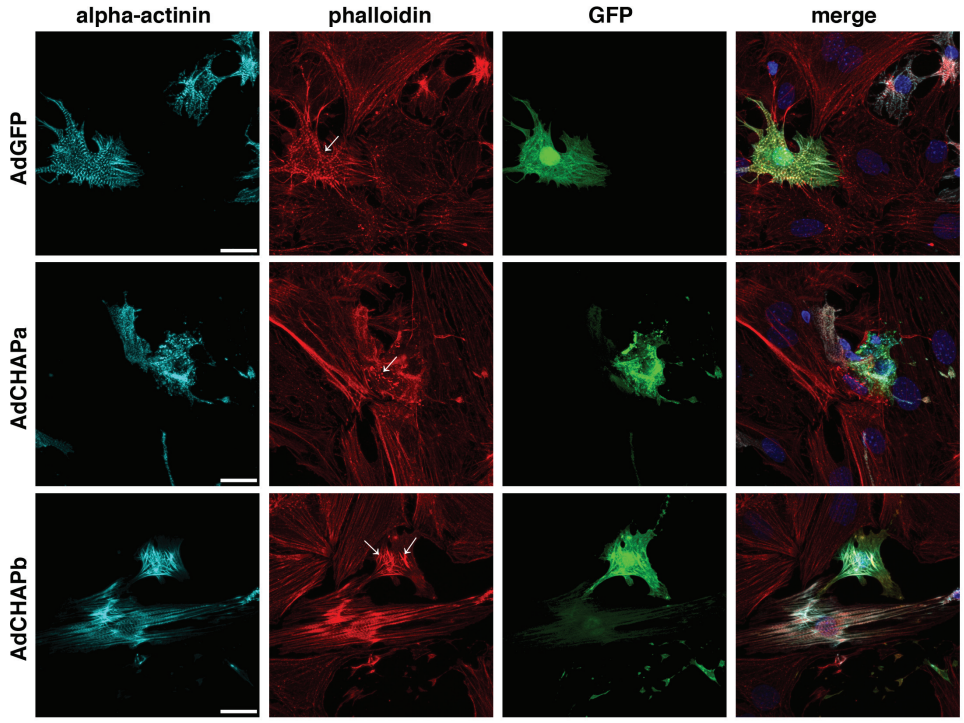

Figure 4: CHAPb, but not CHAPa, overexpression induces F-actin fibers. Mouse cardiomyocytes were infected with AdGFP, AdCHAPa or AdCHAPb and stained for phalloidin (F-actin, red)/CHAP (cyan). Infected cells can be identified by GFP signal (green), nuclei are stained blue, merge images are shown. In AdGFP infected cardiomyocytes (upper panels) phalloidin has a sarcomeric staining pattern. In AdCHAPa infected cardiomyocytes (middle panels) the sarcomeric phalloidin staining is disrupted, while in AdCHAPb infected cardiomyocytes (lower panels) phalloidin stains the fibers.

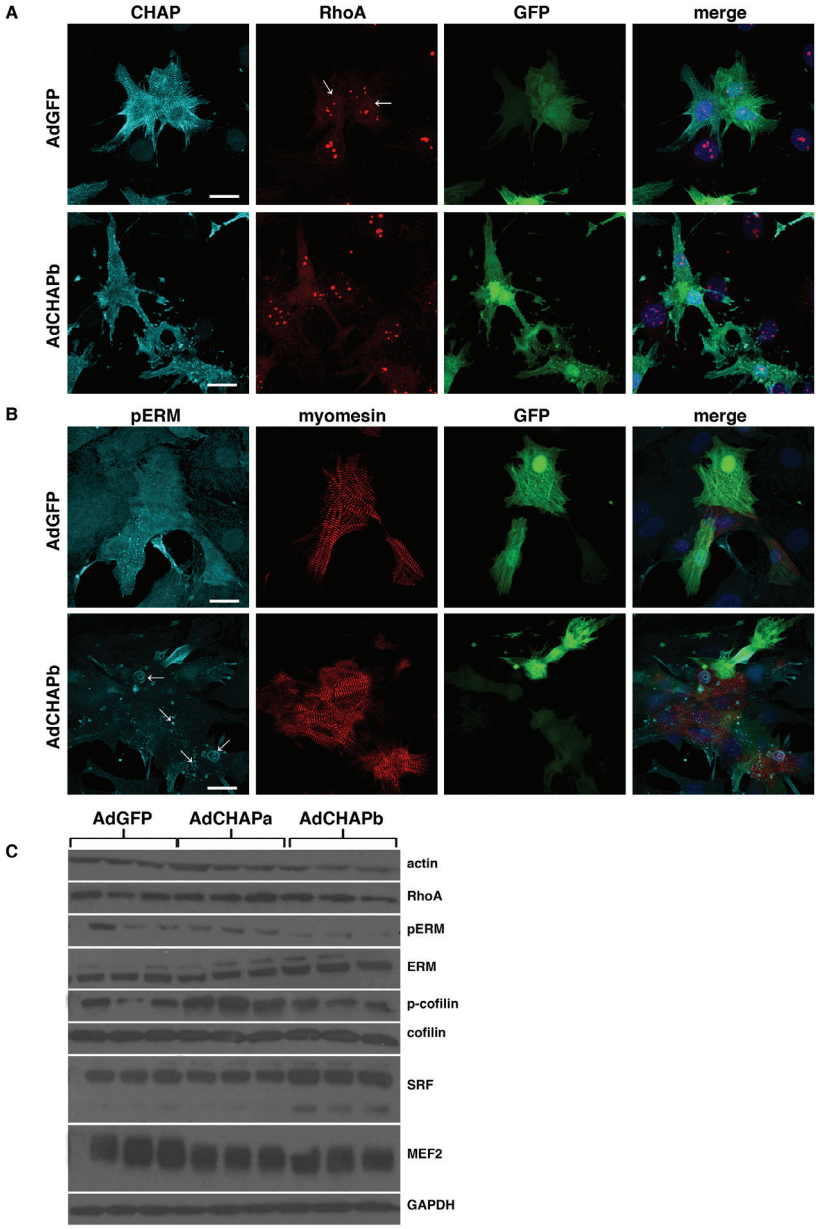

Figure 5: Actin signaling in AdCHAPb infected cells. Mouse cardiomyocytes were infected with AdGFP or AdCHAPb and stained for CHAP (cyan)/ RhoA (red, A) or pERM (cyan)/myomesin (red, B). A) Infected cells can be identified by GFP signal (green), nuclei are stained blue, merge images are shown. In AdGFP infected cardiomyocytes RhoA has a sarcomeric staining pattern (upper panels, arrows), while in AdCHAPb infected cardiomyocytes RhoA sarcomeric expression pattern is lost (lower panels). B) In AdGFP infected cardiomyocytes pERM expression is diffuse (upper panels), whereas in AdCHAPb infected cells pERM localizes at the cell membrane (lower panel, arrows). C) Western blot showing expression of actin, RhoA, pERM, ERM, p-cofilin, cofilin, SRF and MEF2 in mouse cardiomyocytes after infection with AdGFP (n=3), AdCHAPa (n=3) or AdCHAPb (n=3). GAPDH was used as loading control.

Since we previously observed activation of actin-dependent signaling in CHAPb Tg mice (Chapter 4), indicated by upregulated levels of RhoA, actin, α-actinin-2, Ezrin/Moesin/Radixin (ERM), and SRF) at 6 months of age, we investigated whether cellular changes seen in AdCHAPa- or b infected cells were also mediated trough the actin signaling pathway.
In AdGFP infected E17.5 cardiomyocytes RhoA was expressed at high levels in the nucleus in a dotted pattern combined with a sarcomeric expression (Figure 5A, upper panels, arrows). In AdCHAPb infected cells the sarcomeric expression of RhoA was lost, whereas the nuclear expression was not affected (Figure 5A, lower panels). Expression of pERM in AdGFP infected cells was diffuse (Figure 5B, upper panels), whereas expression in AdCHAPb infected cells pERM was expressed at the membrane of the cells (Figure 5B, lower panels, arrows). Next, we investigated the protein expression levels of other components of the actin signaling pathway, actin, RhoA, pERM, ERM, p-cofilin, cofilin, Serum Response Factor (SRF) and Myocyte Enhancer Factor 2 (MEF2) in AdGFP, AdCHAPa and AdCHAPb infected cells. No difference in expression levels were found between the different conditions (Figure 5C). Although, in one experiment, we observed a slight upregulation in p-cofilin in AdCHAPa infected cells and pERM and SRF in AdCHAPb infected cells, these results could not be repeated in other experiments using a different batch of cardiomyocytes. Furthermore, shorter exposure (24 hours) and analysis at a later time point after infection (7 days) did not display any differences between the various conditions (data not shown). These results show that the actin signaling pathway is not directly activated. Although, expression patterns for both RhoA and pERM were affected in AdCHAPb infected cells, compared to the AdGFP control cells, the expression levels of the actin signaling pathway are not affected.

CHAP causes downregulation of hypertrophic markers and translocation of NFAT
In the previous chapter we have seen that CHAPb Tg mice displayed cardiac hypertrophy which was combined with activation of genetic markers of cardiac hypertrophy. In order to study whether CHAP isoforms have a direct effect on the activation of hypertrophic markers we studied hypertrophic markers following adenoviral overexpression. Surprisingly, we observed a clear downregulation of hypertrophy markers. Both ANF (Figure 6A, *Nppa*) and BNP (Figure 6B, *Nppb*) were downregulated to the same extent in AdCHAPa and AdCHAPb cells when compared to AdGFP cells. β-MHC (Figure 6D, *Myh7*) displayed a stronger downregulation in AdCHAPa than in AdCHAPb infected cardiomyocytes. Moreover, α-MHC gene expression (Figure 6C, *Myh6*), which is usually downregulated in cardiac hypertrophy, was increased in AdCHAPa and AdCHAPb infected cells. In addition we also investigated the expression levels of SERCA2A, endogenous *ChapB*, Connexin40, 43 and CollagenI and III, but no differences were detected (data not shown).
The calcineurin-Nuclear Factor of Activated T-cells (NFAT) pathway has been described in many studies as a crucial pathway in the onset and progression of cardiac hypertrophy. Therefore, we investigated the expression of NFAT2c isoform in infected E17.5 cardiomyocytes. Whereas in AdGFP infected cells NFAT2c was localized in the nucleus (Figure 7, upper panels, arrows), in AdCHAPa and AdCHAPb infected cells NFAT2c was translocated to the cytoplasm, suggesting that overexpression of CHAP is able to inhibited calcineurin-NFAT dependent pathway (Figure 7, middle and lower panels, arrow heads).

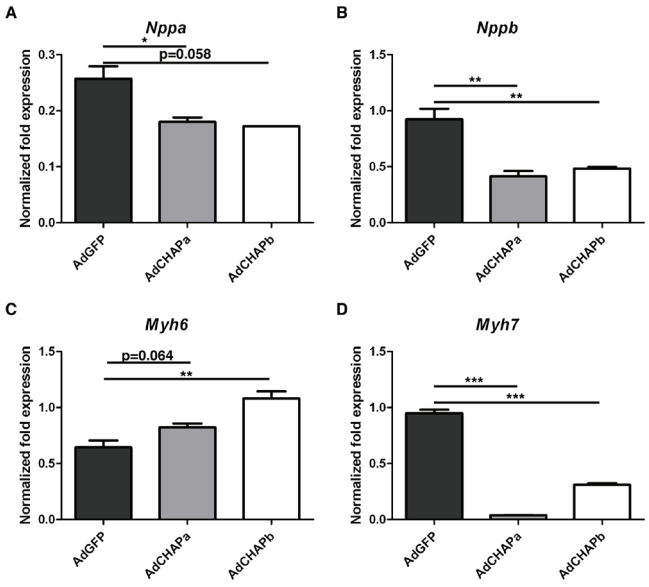

Figure 6: qPCR analysis of hypertrophy markers. Mouse cardiomyocytes were infected with AdGFP (dark grey bars), AdCHAPa (light grey bars) or AdCHAPb (white bars) and expression of *Nppa* (A), *Nppb* (B), *Myh6* (C) or *Myh7* (D) was analyzed. *Gapdh*, *Pgk* and *H2A* were used as internal controls.

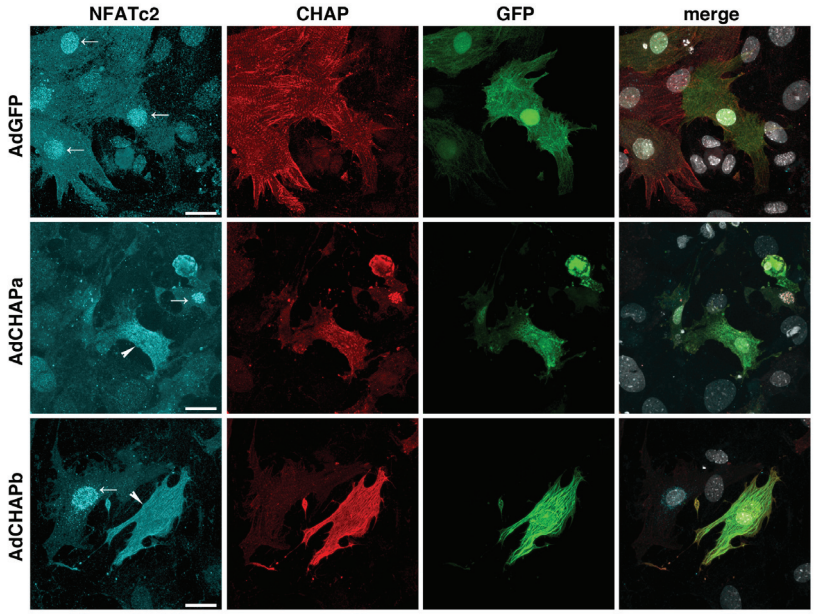

Figure 7: NFATc2 localization is affected by CHAPa and CHAPb. Mouse cardiomyocytes were infected with AdGFP, AdCHAPa or AdCHAPb and stained for NFATc2 (cyan)/CHAP (red). Infected cells can be identified by GFP signal (green), nuclei are stained gray, merge images are shown. In AdGFP infected cells NFATc2 is localized in the nucleus (arrows). In AdCHAPa and AdCHAPb infected cells a cytoplasmic localization for NFATc2 is observed (arrow heads). In some AdCHAPa infected cells both CHAP and NFATc2 were localized in the nucleus and co-staining of these proteins was observed (middle panels).

Discussion

Previously we generated transgenic (Tg) mice that overexpress one of both isoforms of CHAP specifically in the heart. Whereas the CHAPa Tg mice did not develop a phenotype, CHAPb Tg mice developed features of cardiomyopathy, which includes cardiac hypertrophy with diastolic dysfunction. Furthermore, regionalized suppression of connexin 40, formation of stress fibers, increased collagen production and activation of the actin signaling pathway were observed. In order to understand the direct effects of CHAP we have analyzed the *in vitro* function of CHAPa and CHAPb by overexpressing these proteins in mouse cardiomyocytes and skeletal muscle cells (C2C12). To study the effects of CHAP overexpression we developed CHAPa and CHAPb adenoviruses.

CHAPa regulates Z-disc integrity

We have shown in a previous study that CHAPa is co-localized with actin and localizes to the Z-disc as shown by overexpression in rat neonatal cardiomyocytes, suggesting a putative interaction of CHAPa with α-actinin-2, a Z-disc marker[7]. Besides that CHAPa is expressed in adult heart and skeletal muscle (see chapter 2). Therefore, we expect CHAPa to be essential for adult cardiac and skeletal muscle function. Here we generated CHAPa adenovirus to investigate the function of CHAPa *in vitro*. Infection of mouse cardiomyocytes with AdCHAPa resulted in a robust overexpression. Overexpression of CHAPa in E17.5 cardiomyocytes, as wells as skeletal muscle cells (C2C12) resulted in Z-disc disruption. Both, CHAPa and α-actinin-2 were ectopically expressed, while myomesin, a m-band marker, is not affected. Several mouse models have shown that disruption of the Z-disc results in development of dilated cardiomyopathy (DCM). Cypher (Oracle/ZASP) is a PDZ-LIM protein that is expressed in the heart[16, 17] and interacts with α-actinin-2 at the Z-disc[17]. Disruption of Cypher expression leads to the development to DCM in humans, mice and zebrafish[18-22]. Enigma homologue protein (ENH) is another PDZ-LIM protein which interacts with α-actinin-2, Cypher and calsarcin-1[23], and disruption of its expression results in loss of Cypher and calsarcin-1 expression, which leads to development of a DCM phenotype[24]. Cypher and ENH interact with Z-disc protein α-actinin-2 through their PDZ-domains[17, 23]. Given the fact that CHAPa localizes at the Z-disc and bares a PDZ-domain as well, makes it tempting to speculate that the PDZ-domain in CHAPa is responsible for interaction with α-actinin-2. However, CHAPb, the isoform lacking the PDZ-domain, can interact with α-actinin-2 as well[7], therefore it would also possible that the PDZ-domain in CHAPa is not responsible for interaction with α-actinin-2, but interacts with a different subset of cytoskeletal proteins. Therefore, it would be of interest to investigate interaction partners of the CHAPa PDZ-domain by immunoprecipitation experiments. In addition, investigating the function of CHAPa in the cypher/ENH complex would be possible by deleting it conditionally from the heart.

CHAPb induces actin stress fibers

Activation of RhoA promotes both the inhibition of actin depolymerization via the Rho-associated kinase (ROCK)-LIM-kinase-cofilin pathway and the polymerization of actin via profilin, leading to a shift from G-actin to F-actin[25, 26]. Synaptopodin and myopodin are involved in actin bundling via α-actinin [8, 11]and RhoA[12]. Myocardin-related transcription factors (MRTFs) are inhibited by G-actin and depletion of the G-actin pool leads to nuclear localization of the MRTFs. In the nucleus they can act as transcriptional cofactors for SRF[26].

Striated muscle activator of Rho Signaling (STARS) is a novel muscle specific activator of RhoA and regulates thereby the activity of SRF in muscle cells[27, 28]. The transcription of STARS in turn is regulated by MEF2[29]. Cardiac-specific overexpression of MEF2A and MEF2C results in development of DCM[30], whereas knockout models of MEF2A and MEF2D have shown that these factors are involved in the expression of genes regulating contractility and energy metabolism and genes involved in stress-dependent remodeling of the heart, respectively[31, 32]. We have shown the formation of stress fibers by staining for α-actinin-2 by CHAPb *in vivo* (chapter 4). In CHAPb Tg mice the formation of stress fibers was correlated with the induction of actin signaling, demonstrated by the increased expression of RhoA, actin, ERM, cofilin, SRF and MEF2. Furthermore, in hearts of CHAPb Tg mice we showed etopic expression of pERM and RhoA. Here we show, that overexpression of CHAPb *in vitro*, in E17.5 cardiomyocytes as well as skeletal muscle cells, results in similar F-actin. Although we obtained similar results for RhoA and pERM localization, there is no increased expression of the actin signaling pathway. This could imply that the induction of actin signaling is a secondary effect in CHAPb Tg mice. Another explanation could be that members of the actin signaling pathway are already high expressed in embryonic cardiomyocytes. RhoA, for example, is high expressed during development and down regulated in adult heart[33]. Furthermore, the F-actin to G-actin balance might differ between embryonic and adult cardiomyocytes. In addition it maybe possible that stress fiber formation in this model is regulated via a different mechanism, for example via calcineurin-NFAT signaling (see next section).

Role of CHAPa and CHAPb in cardiomyocyte hypertrophy and the calcineurin-NFAT signaling pathway

The calcineurin-NFAT signaling pathway is an essential pathway in the development of hypertrophy. In this pathway the phosphatase calcineurin dephosphorylates NFAT, which leads to its nuclear localization and induction of hypertrophy marker genes like ANF, BNP and β-MHC[3]. Transgenic mice expressing a constitutively active form of the calcineurin catalytic subunit in the heart developed hypertrophy[34], which was mediated by NFATc2 and NFATc3[35, 36]. The nuclear localization of myopodin is regulated by calcineurin as well; phosphorylation dependent binding of 14-3-3 protein to myopodin and subsequent nuclear localization is regulated by PKA and CaMKII, which phosphorylate myopodin and calcineurin, involved in dephosphorylating myopodin[10]. Furthermore, the stability of synaptopodin and its actin-bundling activity is regulated through a similar mechanism in kidney podocytes, in this way linking actin dynamics and calcineurin signaling[37]. It would be of interest to investigate if CHAP stability can be regulated via similar phosphorylation processes. Overexpression of CHAPa or CHAPb in E17.5 cardiomyocytes resulted in translocation of NFATc2 from the nucleus to the cytoplasm. In line with this, the expression levels of the hypertrophy markers were decreased after overexpression of CHAPa or CHAPb. Interestingly, whereas β-MHC was decreased, α-MHC expression on the other hand was increased. Changes in the ratio of both MHC proteins is not only indicative for cardiac hypertrophy, but as well for the maturation phase of cardiac cells, with high levels of α-MHC and low levels of β-MHC. Therefore, decrease in the above mentioned markers may indicate that CHAP either has an anti-hypertrophic activity or a maturation-promoting effect in striated muscle cells. However, these results are in contrast to the observed increase of hypertrophy markers in CHAPb Tg mice (chapter 4), which might indicate an indirect upregulation of these markers in the CHAPb Tg mice. Furthermore, we have to take into account that the cardiomyocytes used for these experiments

are fetal and will have a fetal expression pattern of genes. Therefore, expression of ANF, BNP and β-MHC is expected to be high, whereas α-MHC expression is low. In the adult CHAPb Tg mice however, expression of these markers are low and increase with age. Therefore, the decrease of these factors in AdCHAPa and AdCHAPb infected cardiomyocytes might reflect a morphological change, partially to a more mature or adult phenotype. To investigate the effect of CHAPa and CHAPb on gene expression the use of reporter genes would be an alternative.

Conclusion
Here we show that by *in vitro* overexpressing of CHAPa and CHAPb these two proteins have distinct functions. Whereas CHAPa is involved in Z-disc integrity, CHAPb induces F-actin fibers. It would be interesting to investigate the roles of CHAPa and CHAPb in vivo by conditionally deleting one of both isoforms. For example, we generated floxed CHAP$^{f/+}$ mouse embryonic stem cells (chapter 3) and mouse lines generated from this line can be intercrossed with specific Cre transgenic mice. A CHAPb knock out can be obtained by making use of a α-MHC-Cre or Nkx2.5-Cre, whereas CHAPa can be conditionally deleted by crossing with a tamoxifen inducible mouse line. Furthermore, using a CHAP knock out approach, the role of CHAP in calcineurin-induced hypertrophy can also be investigated *in vivo*, by crossing CHAP knock out mice to calcineurin Tg mice.
In addition, investigating the role of PKA, CaMKII and calcineurin in the stability of CHAP by *in vitro* phosphorylation and inhibition experiments, could clarify the role of calcineurin signaling in CHAP mediated stress fiber formation.

Thus in contrast to what was found in CHAPb Tg mice, overexpression of both CHAPa and CHAPb in vitro leads to downregulation of the hypertrophy markers ANF, BNP and β-MHC, which might be caused by a translocation of NFATc2 from the nucleus to the cytosol upon CHAPa and CHAPb overexpression.

References

(1) Beqqali A, van Eldik W, Mummery C, Passier R. Human stem cells as a model for cardiac differentiation and disease. *Cell Mol Life Sci* 2009 March;66(5):800-13.

(2) Barry SP, Davidson SM, Townsend PA. Molecular regulation of cardiac hypertrophy. *Int J Biochem Cell Biol* 2008;40(10):2023-39.

(3) Wilkins BJ, Molkentin JD. Calcium-calcineurin signaling in the regulation of cardiac hypertrophy. *Biochem Biophys Res Commun* 2004 October 1;322(4):1178-91.

(4) Lange S, Ehler E, Gautel M. From A to Z and back? Multicompartment proteins in the sarcomere. *Trends Cell Biol* 2006 January;16(1):11-8.

(5) Frank D, Kuhn C, Katus HA, Frey N. The sarcomeric Z-disc: a nodal point in signalling and disease. *J Mol Med* 2006 June;84(6):446-68.

(6) Cox L, Umans L, Cornelis F, Huylebroeck D, Zwijsen A. A broken heart: a stretch too far: an overview of mouse models with mutations in stretch-sensor components. *Int J Cardiol* 2008 December 17;131(1):33-44.

(7) Beqqali A, Monshouwer-Kloots J, Monteiro R, Welling M, Bakkers J, Ehler E, Verkleij A, Mummery C, Passier R. CHAP is a newly identified Z-disc protein essential for heart and skeletal muscle function. *J Cell Sci* 2010 April 1;123(Pt 7):1141-50.

(8) Weins A, Schwarz K, Faul C, Barisoni L, Linke WA, Mundel P. Differentiation- and stress-dependent nuclear cytoplasmic redistribution of myopodin, a novel actin-bundling protein. *J Cell Biol* 2001 October 29;155(3):393-404.

(9) Faul C, Huttelmaier S, Oh J, Hachet V, Singer RH, Mundel P. Promotion of importin alpha-mediated nuclear import by the phosphorylation-dependent binding of cargo protein to 14-3-3. *J Cell Biol* 2005 May 9;169(3):415-24.

(10) Faul C, Dhume A, Schecter AD, Mundel P. Protein kinase A, Ca2+/calmodulin-dependent kinase II, and calcineurin regulate the intracellular trafficking of myopodin between the Z-disc and the nucleus of cardiac myocytes. *Mol Cell Biol* 2007 December;27(23):8215-27.

(11) Asanuma K, Kim K, Oh J, Giardino L, Chabanis S, Faul C, Reiser J, Mundel P. Synaptopodin regulates the actin-bundling activity of alpha-actinin in an isoform-specific manner. *J Clin Invest* 2005 May;115(5):1188-98.

(12) Asanuma K, Yanagida-Asanuma E, Faul C, Tomino Y, Kim K, Mundel P. Synaptopodin orchestrates actin organization and cell motility via regulation of RhoA signalling. *Nat Cell Biol* 2006 May;8(5):485-91.

(13) Goncalves MA, van dV, I, Janssen JM, Maassen BT, Heemskerk EH, Opstelten DJ, Knaan-Shanzer S, Valerio D, de Vries AA. Efficient generation and amplification of high-capacity adeno-associated virus/adenovirus hybrid vectors. *J Virol* 2002 November;76(21):10734-44.

(14) Luo J, Deng ZL, Luo X, Tang N, Song WX, Chen J, Sharff KA, Luu HH, Haydon RC, Kinzler KW, Vogelstein B, He TC. A protocol for rapid generation of recombinant adenoviruses using the AdEasy system. *Nat Protoc* 2007;2(5):1236-47.

(15) Knaan-Shanzer S, van dV, I, Havenga MJ, Lemckert AA, de Vries AA, Valerio D. Highly efficient targeted transduction of undifferentiated human hematopoietic cells by adenoviral vectors displaying fiber knobs of subgroup B. *Hum Gene Ther* 2001 November 1;12(16):1989-2005.

(16) Passier R, Richardson JA, Olson EN. Oracle, a novel PDZ-LIM domain protein expressed in heart and skeletal muscle. *Mech Dev* 2000 April;92(2):277-84.

(17) Zhou Q, Ruiz-Lozano P, Martone ME, Chen J. Cypher, a striated muscle-restricted PDZ and LIM domain-containing protein, binds to alpha-actinin-2 and protein kinase C. *J Biol Chem* 1999 July 9;274(28):19807-13.

(18) Zhou Q, Chu PH, Huang C, Cheng CF, Martone ME, Knoll G, Shelton GD, Evans S, Chen J. Ablation of Cypher, a PDZ-LIM domain Z-line protein, causes a severe form of congenital myopathy. *J Cell Biol* 2001 November 12;155(4):605-12.

(19) Zheng M, Cheng H, Li X, Zhang J, Cui L, Ouyang K, Han L, Zhao T, Gu Y, Dalton ND, Bang ML, Peterson KL, Chen J. Cardiac-specific ablation of Cypher leads to a severe form of dilated cardiomyopathy with premature death. *Hum Mol Genet* 2009 February 15;18(4):701-13.

(20) Cheng H, Zheng M, Peter AK, Kimura K, Li X, Ouyang K, Shen T, Cui L, Frank D, Dalton ND, Gu Y, Frey N, Peterson KL, Evans SM, Knowlton KU, Sheikh F, Chen J. Selective deletion of long but not short Cypher isoforms leads to late-onset dilated cardiomyopathy. *Hum Mol Genet* 2011 May 1;20(9):1751-62.

(21) Vatta M, Mohapatra B, Jimenez S, Sanchez X, Faulkner G, Perles Z, Sinagra G, Lin JH, Vu TM, Zhou Q, Bowles KR, Di LA, Schimmenti L, Fox M, Chrisco MA, Murphy RT, McKenna W, Elliott P, Bowles NE, Chen J, Valle G, Towbin JA. Mutations in Cypher/ZASP in patients with dilated cardiomyopathy and left ventricular non-compaction. *J Am Coll Cardiol* 2003 December 3;42(11):2014-27.

(22) van der Meer DL, Marques IJ, Leito JT, Besser J, Bakkers J, Schoonheere E, Bagowski CP. Zebrafish cypher is important for somite formation and heart development. *Dev Biol* 2006 November 15;299(2):356-72.

(23) Nakagawa N, Hoshijima M, Oyasu M, Saito N, Tanizawa K, Kuroda S. ENH, containing PDZ and LIM domains, heart/skeletal muscle-specific protein, associates with cytoskeletal proteins through the PDZ domain. *Biochem Biophys Res Commun* 2000 June 7;272(2):505-12.

(24) Cheng H, Kimura K, Peter AK, Cui L, Ouyang K, Shen T, Liu Y, Gu Y, Dalton ND, Evans SM, Knowlton KU, Peterson KL, Chen J. Loss of enigma homolog protein results in dilated cardiomyopathy. *Circ Res* 2010 August 6;107(3):348-56.

(25) Maekawa M, Ishizaki T, Boku S, Watanabe N, Fujita A, Iwamatsu A, Obinata T, Ohashi K, Mizuno K, Narumiya S. Signaling from Rho to the actin cytoskeleton through protein kinases ROCK and LIM-kinase. *Science* 1999 August 6;285(5429):895-8.

(26) Olson EN, Nordheim A. Linking actin dynamics and gene transcription to drive cellular motile functions. *Nat Rev Mol Cell Biol* 2010 May;11(5):353-65.

(27) Arai A, Spencer JA, Olson EN. STARS, a striated muscle activator of Rho signaling and serum re sponse factor-dependent transcription. *J Biol Chem* 2002 July 5;277(27):24453-9.

(28) Kuwahara K, Barrientos T, Pipes GC, Li S, Olson EN. Muscle-specific signaling mechanism that links actin dynamics to serum response factor. *Mol Cell Biol* 2005 April;25(8):3173-81.

(29) Kuwahara K, Teg Pipes GC, McAnally J, Richardson JA, Hill JA, Bassel-Duby R, Olson EN. Modula tion of adverse cardiac remodeling by STARS, a mediator of MEF2 signaling and SRF activity. *J Clin Invest* 2007 May;117(5):1324-34.

(30) Xu J, Gong NL, Bodi I, Aronow BJ, Backx PH, Molkentin JD. Myocyte enhancer factors 2A and 2C induce dilated cardiomyopathy in transgenic mice. *J Biol Chem* 2006 April 7;281(14):9152-62.

(31) Kim Y, Phan D, van RE, Wang DZ, McAnally J, Qi X, Richardson JA, Hill JA, Bassel-Duby R, Olson EN. The MEF2D transcription factor mediates stress-dependent cardiac remodeling in mice. *J Clin Invest* 2008 January;118(1):124-32.

(32) Naya FJ, Black BL, Wu H, Bassel-Duby R, Richardson JA, Hill JA, Olson EN. Mitochondrial deficiency and cardiac sudden death in mice lacking the MEF2A transcription factor. *Nat Med* 2002 November;8(11):1303-9.

(33) Ahuja P, Perriard E, Pedrazzini T, Satoh S, Perriard JC, Ehler E. Re-expression of proteins involved in cytokinesis during cardiac hypertrophy. *Exp Cell Res* 2007 April 1;313(6):1270-83.

(34) Molkentin JD, Lu JR, Antos CL, Markham B, Richardson J, Robbins J, Grant SR, Olson EN. A calcineurin-dependent transcriptional pathway for cardiac hypertrophy. *Cell* 1998 April 17;93(2):215-28.

(35) Wilkins BJ, De Windt LJ, Bueno OF, Braz JC, Glascock BJ, Kimball TF, Molkentin JD. Targeted disruption of NFATc3, but not NFATc4, reveals an intrinsic defect in calcineurin-mediated cardiac hypertrophic growth. *Mol Cell Biol* 2002 November;22(21):7603-13.

(36) Bourajjaj M, Armand AS, da Costa Martins PA, Weijts B, van der NR, Heeneman S, Wehrens XH, De Windt LJ. NFATc2 is a necessary mediator of calcineurin-dependent cardiac hypertrophy and heart failure. *J Biol Chem* 2008 August 8;283(32):22295-303.

(37) Faul C, Donnelly M, Merscher-Gomez S, Chang YH, Franz S, Delfgaauw J, Chang JM, Choi HY, Campbell KN, Kim K, Reiser J, Mundel P. The actin cytoskeleton of kidney podocytes is a direct target of the antiproteinuric effect of cyclosporine A. *Nat Med* 2008 September;14(9):931-8.